

画像の局所的な傾きを用いた高精度のWaDi補間法

High Accuracy WaDi Image Interpolation with Local Gradient Features

○袁 帥*, 阿部 正英*, 田口 亮**, 川又 政征*

Shuai Yuan*, Masahide Abe*, Akira Taguchi**, Masayuki Kawamata*

*東北大学大学院工学研究科電子工学専攻, **武蔵工業大学電気電子工学科

*Department of Electronic Engineering, Graduate School of Engineering,
Tohoku University

**Department of Electrical and Electronic Engineering,
Musashi Institute of Technology

キーワード : 補間法(interpolation), warped distance, 局所的な非対称性(local asymmetry feature), 局所的な傾き(local gradient feature)

連絡先 : 〒980-8579 仙台市青葉区荒巻字青葉6-6-05 東北大学大学院 工学研究科 電子工学専攻 川又研究室
袁帥, Tel.: 022-795-7095, Fax.: 022-263-9169, E-mail: yuan@mk.ecei.tohoku.ac.jp

1. Introduction

Image interpolation is a prime technique in image processing. It is used in many important applications such as digital high-definition television, big screen display, copy and print machine, medical imaging, end-user equipment and so on.

The conventional image linear interpolations (e.g., the bilinear and bicubic interpolations [1]) are used widely in many applications. However, the conventional linear interpolations have a serious blurring problem, because they ignore the features of the image pixel data, such as the frequency features, the edge features, the features under multi-resolution and so on. For solving the blurring problem in image interpolation, various resolution

enhancement (RE) interpolation algorithms were proposed. Some of the RE interpolation algorithms [2], [3] use multiresolution pyramid representations of a low-resolution image to calculate an interpolated high-resolution image. In [2], the Laplacian pyramid is used for predicting the high frequency components. In [3], a wavelet-based interpolation is presented. Another popular type of the RE interpolation algorithms [4]-[7] needs a sequence of low-resolution images for producing an interpolated high-resolution image. Since the interpolations based on multi-resolution pyramids or multi-image datas need heavy computations, they can not replace the bilinear or bicubic interpolations, in particular when the computational simplicity is wanted. For example, in many cases the interpola-

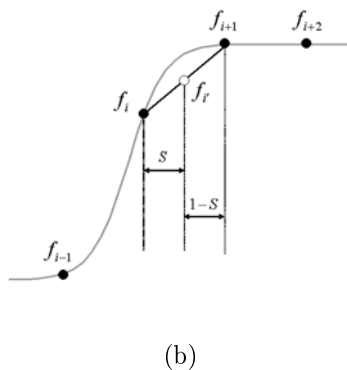
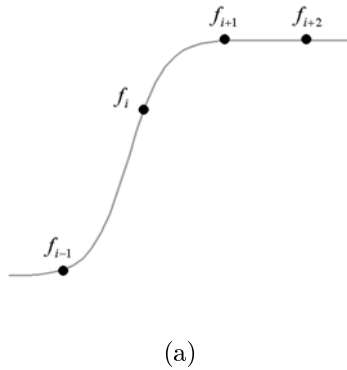


Fig. 1 Bilinear interpolation. (a) An edge model. (b) Bilinear interpolation for up-sampling.

tor is included in end-user equipment, which should have low cost and computational simplicity.

For improving the performance of the conventional linear interpolations, the conventional WaDi technique was proposed by Ramponi in [8]. Since the WaDi technique can reduce the interpolation error and has a simple computation structure, it is expected to replace the conventional linear interpolations in many applications. The conventional WaDi technique is based on the local asymmetry features of image edges. We know that the local gradient features are one kind of the important features of image edges as well as the local asymmetry features. In this paper we adopt these two kinds of features in the proposed WaDi bilinear interpolation method, more image details of which are displayed than those of the conventional WaDi in the interpolated images.

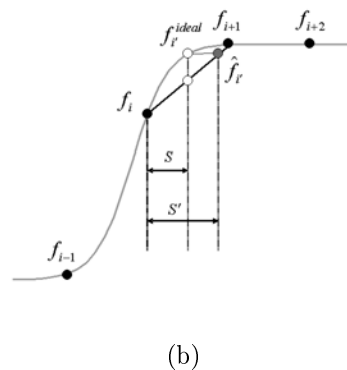
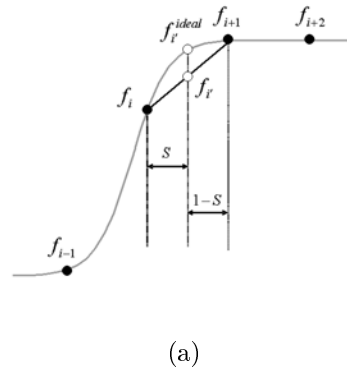


Fig. 2 Ideal interpolation value f_r^{ideal} , (a) bilinear interpolation value f_r and (b) WaDi interpolation value \hat{f}_r .

This paper is organized as follows. The conventional WaDi interpolation is reviewed in Section 2.1. The local gradient features of digital images are described in Section 2.2. The proposed WaDi interpolation method is presented in Section 2.3. Some experimental results are given in Section 3. Finally, the conclusion is included in Section 4.

2. WaDi Interpolation With Local Gradient Features

Since any lowpass effect in the courses when we obtain natural images will change step edges into sigmoidal edges, we use a sigmoidal function as a model for image edges. The conventional linear interpolations need an up-sampling distance s to estimate the unknown pixels for up-sampling. For

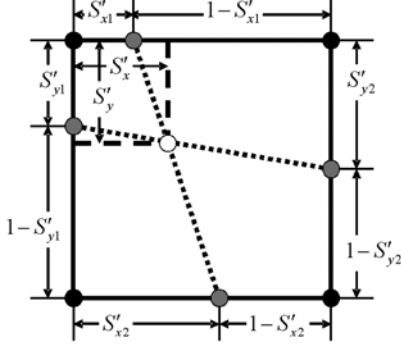


Fig. 3 Relationship between 2-D warped distances and 1-D warped distances.

an edge model the bilinear interpolation is shown in Fig. 1.

At the position i' , the bilinear interpolation estimates the value of the interpolated pixel as

$$f_{i'} = (1 - s)f_i + sf_{i+1}, \quad (1)$$

where the distance s is defined by $s = i' - i$. However, from Fig. 1 we know that the bilinear interpolated value $f_{i'}$ at the position i' does not correctly represent the real value $f_{i'}^{ideal}$. This reason makes the interpolated images using the bilinear interpolation blurred.

2.1 Conventional WaDi Interpolation

For obtaining the ideal interpolated value $f_{i'}^{ideal}$, the WaDi interpolation uses the WaDi s' in place of the distance s in the conventional linear interpolations. Fig. 2 shows how the WaDi s' works. Thus, we can find s' with

$$\begin{aligned} \hat{f}_{i'} &= (1 - s')f_i + s'f_{i+1} \\ &= f_{i'}^{ideal}. \end{aligned} \quad (2)$$

The WaDi s' depends on image local features. Utilizing the local asymmetry features, the conventional WaDi interpolation defines s' as

$$s' = s - kAs(1 - s), \quad (3)$$

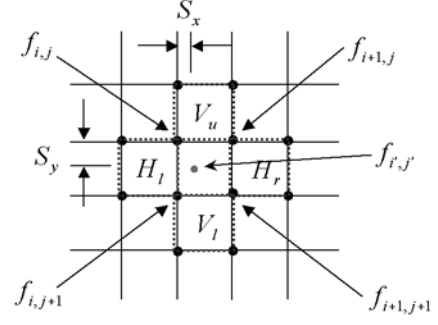


Fig. 4 Pixel masks around the interpolated pixel.

where A is the local asymmetry feature defined by

$$A = \frac{|f_{i+1} - f_{i-1}| - |f_{i+2} - f_i|}{L - 1}, \quad (4)$$

where $L = 256$ for 8-bit luminance images, and then A is limited in the range $[-1, 1]$. The positive parameter k decides the warping level. When k is large, s' may be outside of the range $[0, 1]$. Since s' must be kept in $[0, 1]$ in real images, the outside-range s' will be clipped to 0 or 1.

Two-dimensional (2-D) WaDi can be computed from one-dimensional (1-D) WaDis. Fig. 3 shows the relationship between the 2-D WaDi and the 1-D WaDis. Therefore, we have the equations for the 2-D WaDi computation as

$$s'_x = \frac{s'_{x1} + (s'_{x2} - s'_{x1})s'_{y1}}{1 - (s'_{y2} - s'_{y1})(s'_{x2} - s'_{x1})} \quad (5)$$

$$s'_y = \frac{s'_{y1} + (s'_{y2} - s'_{y1})s'_{x1}}{1 - (s'_{y2} - s'_{y1})(s'_{x2} - s'_{x1})}. \quad (6)$$

2.2 Local Gradient Features

In digital images, the local gradient features are also one kind of the important features. In [9], using the local gradient features around the interpolated pixel $f_{i',j'}$, four local gradient weights are proposed by Hwang. The four local gradient weights, H_l , H_r , V_u and V_l are generated from the four pixel masks around the interpolated pixel, where the four

masks are shown in Fig. 4 with the dotted line blocks. The local gradient weights H_l , H_r , V_u and V_l are defined as

$$\begin{aligned} H_l &= \frac{1}{\sqrt{1 + \alpha(|f_{i,j} - f_{i-1,j}| + |f_{i,j+1} - f_{i-1,j+1}|)}} \\ H_r &= \frac{1}{\sqrt{1 + \alpha(|f_{i+1,j} - f_{i+2,j}| + |f_{i+1,j+1} - f_{i+2,j+1}|)}} \\ V_u &= \frac{1}{\sqrt{1 + \alpha(|f_{i,j} - f_{i,j-1}| + |f_{i+1,j} - f_{i+1,j-1}|)}} \\ V_l &= \frac{1}{\sqrt{1 + \alpha(|f_{i,j+1} - f_{i,j+2}| + |f_{i+1,j+1} - f_{i+1,j+2}|)}} \end{aligned}$$

where the parameter α is in the range of $[0, 1]$.

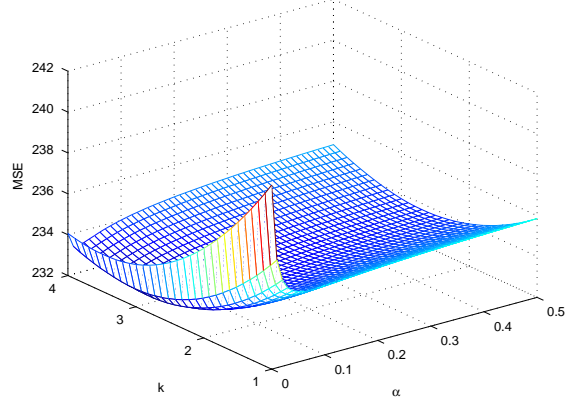
2.3 Proposed High Accuracy WaDi Interpolation

From [9], we know that the local gradient weights can be used for the bilinear interpolation as

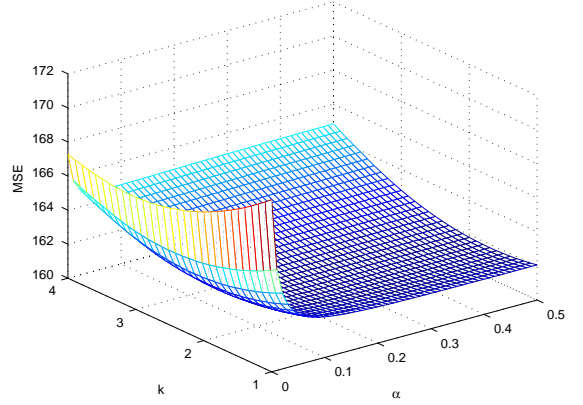
$$\begin{aligned} f_{i',j'}^g &= \frac{H_l(1-s_x)}{H_l(1-s_x) + H_r s_x} \cdot \frac{V_u(1-s_y)}{V_u(1-s_y) + V_l s_y} \cdot f_{i,j} \\ &+ \frac{H_r s_x}{H_l(1-s_x) + H_r s_x} \cdot \frac{V_u(1-s_y)}{V_u(1-s_y) + V_l s_y} \cdot f_{i+1,j} \\ &+ \frac{H_l(1-s_x)}{H_l(1-s_x) + H_r s_x} \cdot \frac{V_l s_y}{V_u(1-s_y) + V_l s_y} \cdot f_{i,j+1} \\ &+ \frac{H_r s_x}{H_l(1-s_x) + H_r s_x} \cdot \frac{V_l s_y}{V_u(1-s_y) + V_l s_y} \cdot f_{i+1,j+1}. \end{aligned} \quad (7)$$

Using both the local asymmetry and the local gradient features, the proposed WaDi interpolation replaces s_x and s_y in (7) with the conventional WaDi s'_x and s'_y , respectively. Then, we can get

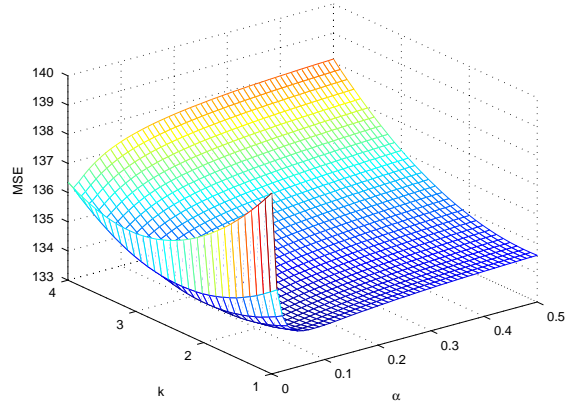
$$\begin{aligned} f_{i',j'}^p &= \frac{H_l(1-s'_x)}{H_l(1-s'_x) + H_r s'_x} \cdot \frac{V_u(1-s'_y)}{V_u(1-s'_y) + V_l s'_y} \cdot f_{i,j} \\ &+ \frac{H_r s'_x}{H_l(1-s'_x) + H_r s'_x} \cdot \frac{V_u(1-s'_y)}{V_u(1-s'_y) + V_l s'_y} \cdot f_{i+1,j} \\ &+ \frac{H_l(1-s'_x)}{H_l(1-s'_x) + H_r s'_x} \cdot \frac{V_l s'_y}{V_u(1-s'_y) + V_l s'_y} \cdot f_{i,j+1} \end{aligned}$$



(a)



(b)



(c)

Fig. 5 MSE variance. (a) “Airplane” image with different parameter sets. (b) “Lenna” image with different parameter sets. (c) “Peppers” image with different parameter sets.



(a)



(b)



(b)



(c)



(d)



(e)

Fig. 6 Experimental interpolated images. (a) Bilinear interpolated “Pepper” image (MSE=143.2). (b) Edge components of (a) after the Laplacian filtering. (c) Conventional WaDi interpolated “Pepper” image (MSE=135.6). (d) Edge components of (c) after the Laplacian filtering. (e) Proposed WaDi interpolated “Pepper” image (MSE=135.6). (f) Edge components of (e) after the Laplacian filtering.

Table 1 The minimized MSE values ($128 \times 128 \rightarrow 256 \times 256$).

Image	Bilinea	Conventional WaDi	Proposed WaDi
Airplane	247.8	233.8	232.4
Cameraman	325.1	312.7	310.4
Lenna	174.1	166.5	161.9
Pepper	143.2	135.6	133.9
Lighthouse	392.0	376.1	374.6
Clock	142.6	130.3	129.2
Tiffany	158.4	154.1	153.4
Couple	70.4	67.2	66.9

$$+ \frac{H_r s'_x}{H_l(1-s'_x) + H_r s'_x} \cdot \frac{V_l s'_y}{V_u(1-s'_y) + V_l s'_y} \cdot f_{i+1,j+1}. \quad (8)$$

Then, the proposed WaDis can be easily written as

$$s_x^{p'} = \frac{H_r s'_x}{H_l(1-s'_x) + H_r s'_x}$$

$$s_y^{p'} = \frac{V_l s'_y}{V_u(1-s'_y) + V_l s'_y},$$

and $f_{i',j'}^p$ can also be easily written as

$$f_{i',j'}^p = (1-s_x^{p'})(1-s_y^{p'})f_{i,j} + s_x^{p'}(1-s_y^{p'})f_{i+1,j} \\ + (1-s_x^{p'})s_y^{p'}f_{i,j+1} + s_x^{p'}s_y^{p'}f_{i+1,j+1}. \quad (9)$$

3. Experimental Results

To do a quantitative evaluation of the proposed WaDi interpolation, we use the “imresize(I, 0.5, bilinear)” of matlab to lowpass filter the different well-known test images (256×256) and subsample the lowpass filtered images to 1/2 times of their original size. Then, the subsampled images are interpolated to their original size using the bilinear,

the proposed WaDi and the conventional WaDi interpolations. The minimized MSE values for each interpolation method are presented in Table I. The results in Table I show that for all the test images the proposed WaDi interpolation can get better interpolated accuracy than that of the conventional WaDi interpolation.

Using the conventional WaDi interpolation, when the parameter k is large the interpolated images are seen to be sharp. When the parameter k increases, the MSE also increases fast, because not only the high frequency components (edges) but also the low frequency components of an image are affected easily by the parameter k . In the proposed WaDi interpolation we have the other parameter α . Using the proposed WaDi interpolation we show the MSE variance graphs of the “Airplane”, “Lenna” and “Pepper” images with different parameter sets of k and α in Fig. 5. When the parameter α is large, the interpolated images are also shown sharp. Fig. 5 shows us that the increment of the parameter α affects the MSE variance little, and this feature means that using the proposed WaDi interpolation we can sharpen the interpolated images by increasing the parameter α only with a little MSE increment. The interpolated “Pepper” images are shown in Fig. 6, where the proposed WaDi and the conventional WaDi interpolated images are under the same MSE value. From the edge components of the proposed WaDi interpolated, the conventional WaDi interpolated and the bilinear interpolated images in Fig. 6, we can see that the proposed WaDi interpolation can obtain more edge details in the interpolated images than those of the conventional WaDi and the bilinear interpolations.

4. Conclusion

The proposed WaDi interpolation in this paper uses both the local asymmetry features and the local gradient features of an image to compute the warped distance. In this way more image local information is used to estimate the interpolated pixels than that in the conventional WaDi interpolation.

Experiment results show that:

1) Using optimum parameters k and α , the MSE values of the proposed WaDi interpolated images made smaller than those of the conventional WaDi interpolated images;

2) Under the same MSE values, the proposed WaDi interpolated images display more edge details than those in the conventional WaDi interpolated images.

参考文献

- 1) W. K. Pratt, *Digital Image Processing*, New York: Wiley, 1991.
- 2) H. Greenspan, C. H. Anderson and S. Akber, "Image enhancement by nonlinear extrapolation in frequency space," *IEEE Trans. on Image Processing*, vol. 9, no. 6, pp. 1035-1048, June 2000.
- 3) W. K. Carey, D. B. Chuang and S. S. Hemami, "Regularity-preserving image interpolation," *IEEE Trans. on Image Processing*, vol. 8, no. 9, pp. 1293-1297, September 1999.
- 4) S. P. Kim and W. Y. Su, "Recursive high resolution reconstruction of blurred multiframe images," *IEEE Trans. on Image Processing*, vol. 2, pp. 534-539, October 1993.
- 5) R. Hardie, K. Barnard. and E. Armstrong, "Joint map registration and high resolution image estimation using a sequence of undersampled measured images," *IEEE Trans. on Image Processing*, vol. 6, pp. 1621-1632, December 1997.
- 6) N. R. Shah and A. Zakhor, "Resolution enhancement of color video sequences," *IEEE Trans. on Image Processing*, vol. 8, no. 6, pp. 879-885, June 1999.
- 7) B. C. Tom and A. K. Katsaggelos, "Resolution enhancement of monochrome and color video using motion compensation," *IEEE Trans. on Image Processing*, vol. 10, no. 2, pp. 278-287, February 2001.
- 8) G. Ramponi, "Warped distance for space-variant linear image interpolation," *IEEE Trans. on Image Processing*, vol. 8, no. 5, pp. 629-639, May 1999.
- 9) J. W. Hwang and H. S. Lee, "Adaptive image interpolation based on local gradient features," *IEEE Signal Processing Letters*, vol. 11, no. 3, pp. 359-362, March 2004.